Journal of Metals, Materials and Minerals, 34(2), 1966, 2024

Fabrication of porous geopolymers utilizing aluminum wastes as foaming agent

Siriwan CHOKKHA[1], Jiratchaya AYAWANNA[1], Anurat POOWANCUM[1,*], Thanasak SINGLAEM[1], and Pusit MITSOMWANG[2]

[1] *School of Ceramic Engineering, Institute of Engineering, Suranaree University of Technology, Nakhon Ratchasima, Thailand*
[2] *School of Metallurgical Engineering, Institute of Engineering, Suranaree University of Technology, Nakhon Ratchasima, Thailand*

***Corresponding author e-mail**: anurat@sut.ac.th

Received date:
17 February 2024
Revised date
26 March 2024
Accepted date:
23 April 2024

Keywords:
Porous geopolymer;
Aluminum salt slag;
Geopolymer;
Porous materials;
Foaming agent

Abstract

Porous geopolymers (PG) are attractive due to their simple fabrication and diverse applications. This work presents a method for fabricating PG by using aluminum salt slag (ASS) as a foaming agent and metakaolin (MK) as the precursor. Sodium silicate (Na_2SiO_3) and sodium hydroxide (NaOH) are used as alkali activator solutions. The results show that the PG is fabricated by using the sequence mixing method. ASS was milled to a size of 4 μm, then mixed with an NaOH solution for 30 min. After that, MK and Na_2SiO_3 solution were added. The weight ratio of Na_2SiO_3/NaOH and solid/liquid was 2.0 and 0.6, respectively. The 7-day cured PG with 5 wt% ASS achieves a strength of 15 MPa, which is close to the minimum requirement of Portland cement of 19 MPa. PG strength decreases, while setting time and pore size increase with increasing ASS content. The knowledge of this work enables the utilization of ASS as a valuable geopolymer foaming agent.

1. Introduction

Aluminum is one of the most used metals in the world [1]. The demand for aluminum is on the rise annually [2]. A rapid demand growth of aluminum leads to an increase in aluminum salt slag (ASS) waste, which is generated during the secondary aluminum recycling process [3]. Dai and Apelian [4] have reported that the annual amount of ASS may exceed 5 million tons. ASS is mainly composed of aluminum (Al), alumina (Al_2O_3), aluminum nitride (AlN), salt and other oxides [5]. ASS is unusable for engineering applications and is typically disposed of in landfills, which is detrimental to the ecosystem [6-8]. Numerous studies have been conducted to find a solution for managing ASS waste. The use of ASS in construction applications has been reported. Stiffness and corrosion resistance of asphalt is improved by using ASS as a filler [9]. Dai and Apelian [10] reported that a 40% increase in flexural strength, and a 15% increase in compressive strength by using ASS as the filler in the mortar between 10 wt% to 20 wt% [10]. One effective way is to utilize ASS as a valuable material, specifically as a foaming agent for the development of the porous geopolymer (PG).

A geopolymer is a green material, is a cement replacement material, and is synthesized by mixing aluminosilicate materials with an alkali activator solution. Aluminosilicate materials are mainly composed of alumina (Al_2O_3) and silica (SiO_2) such as fly ash, metakaolin (MK), and slag [11-13]. Alkali activator solution is usually a combination of alkali hydroxide (NaOH or KOH) and alkali silicate (Na_2SiO_3 or K_2SiO_3) [11-13]. The geopolymer synthesizing process emits a small amount of carbon dioxide (CO_2) gas, which is a major cause of global warming and is released in large quantities by the cement production process. Currently, the development of geopolymer materials is widely studied [14]. Many parameters effect on property of geopolymer have been reported. Concentration of NaOH affects porosity and compressive strength of geopolymer. Compressive strength and denser microstructure increased with higher NaOH concentration [15]. Higher concentrations enhanced dissolution and formation of reaction products resulted in denser matrices and smaller average pore diameters [15]. Prasanphan *et al.* suggested that the highest compressive strength of MK-based geopolymer was obtained with a NaOH concentration of 10 M [15]. The Na_2SiO_3 to NaOH ratio, also known is a key parameter that impacts the engineering efficiency of geopolymer [16]. Mousavinejad and Sammak reported that an increasing of Na_2SiO_3 to NaOH ratio leads to the production of a silica-rich geopolymer network and accelerates the geopolymerization process result in enhancing the mechanical strength [17]. The solid to liquid ratio influences the compressive strength, density, and workability efficiency of geopolymers. Lower solid to liquid ratios can lead to improved workability efficiency. The compressive strength of metakaolin-based geopolymers at 30 MPa to 60 MPa for solid to liquid ratio of 0.6 to 1.1 has ever been reported [18]. Curing conditions are one of the important parameters that affect the properties of PG. Curing at higher temperatures, leads to a decrease in porosity in geopolymers [19]. Liu et al. showed that curing at 40°C demonstrated the best mechanical properties, with dense microstructures [20]. Yilmaz *et al.* reported that curing times were more effective than curing temperatures in terms of porosity values, which decreased as the curing times increased [21]. Extended curing periods leading to denser microstructures, reduce porosity and enhance mechanical properties [19].

The PG is classified as porous material, and can be used for various applications including ion or gas adsorption, water purification, catalyst support, thermal insulation, lightweight parts, pH buffering, and drug release [22,23]. The synthesis of PG can be accomplished by a variety of techniques, including direct foaming, sacrificial template method, freeze casting, replica method, sacrificial filler method, gel casting [14,22]. Direct foaming is the most popular due to it is simplicity method. The commonly used foaming agents are aluminum [24-26], hydrogen peroxide [27,28] and silicon or silica fume [14,22,29]. Zoude *et al*. [30] developed 3D-printed metakaolin-based porous geopolymers (MK-PGs) using aluminum powder as a foaming agent. The MK-PGs have a compressive strength of 2.0 ± 0.5 MPa and a total porosity of 71.27 ± 0.75 vol%. Sornlar *et al.* [31] fabricated the MK-PGs by using sodium lauryl ether sulfate (SLES) as the foaming agent. The results show that the porosity increased with the increased amount of the SLES leading to the decrease of compressive strength. The compressive strength of samples containing SLES of 0, 5, 10, and 15 wt% are 48.80 ± 3.15, 14.82 ± 0.50, 7.69 ± 0.24, and 4.69 ± 0.97 MPa, respectively. Sanguanpak *et al.* [32] developed MK-PGs using an air foam to generate the pores. The researchers found that varying air foam content affected the physical and mechanical properties of geopolymers. With an increase in air foam content from 0% to 15 wt%, the apparent porosity increased from 32.37% to 71.31%. On the other hand, the compressive strength decreased from 41.46 MPa to 3.28 MPa. Jaya *et al.* [33] investigated the combination effect of foaming agent (H_2O_2) and surfactant (polyethylene glycol-sorbitan monooleate) on properties of MK-PGs. The results show that incorporation of foaming agent and surfactant reduced the compressive strength, while increasing the porosity of MK-PGs. By adding foaming agent of 0.25% and surfactant of 1% produced MK-PGs foam with acceptable compressive strength of 6.0 MPa with porosity of 36%. Fiset et al. [34] fabricated MK-PGs using hydrogen peroxide and canola oil as the foaming agent and surfactant, respectively. The pores of the MK-PGs were infused with an unsaturated polyester resin (UPE). The results showed that the pore diameter and size distribution are controlled by the synergistic effects of foaming agent and surfactant. In addition, the compressive strength of the MK-PGs improved up to 40 times with the incorporation of the UPE. Numerous studies have investigated the effect of foaming agent content on the properties of PG. The optimal amount of foaming agent depends on the type of foaming agent used and the intended application of the PG. Xu *et al.* [35] reported the effect of hydrogen peroxide on porosity and compressive strength of PG. By adding hydrogen peroxide in the range of 1% to 3.5%, the obtained PG contain porosity and compressive strength in the range of 32.3% to 63.1% and 44.81 MPa to 3.2 MPa, respectively. This strength is possible to use as the lightweight geopolymer foams. Liu *et al.* [36] developed PG using fly ash as the precursor and silica fume as the foaming agent. With the addition of 15% to 45% silica fume, the resulting PG exhibits porosity in the range of around 40% to 25% and compressive strength around 20 MPa to 7 MPa. These properties make it suitable for use as sound insulation. Wattanasiriwech *et al.* [37] developed geopolymer foams using aluminum powder as the foaming agent. The geopolymer foams exhibit porosity of around 45% with 0.1% aluminum content. This porosity increases to 52% at 0.2% to 0.3% aluminum content. The compressive strength of the geopolymer foam was in the range of 0.9 MPa to 4.35 MPa, which was suitable for use as bricks, and fire-resistant panels. Jaya et al. [38] added hydrogen peroxide in the range of 0.25 wt% to 1.25 wt% to MK-based geopolymer to produce geopolymer foam (GF). The GF exhibits acceptable compressive strength ranging from 0.4 MPa to 6 MPa. Masi *et al.* [39] synthesized light weight geopolymers (LWG) using aluminum powder and hydrogen peroxide solution as foaming agents. By adding aluminum powder in the range of 0.01 wt% to 0.05 wt% to the fly ash-based geopolymer, the LWG exhibits compressive strength values between 1.7 MPa and 2.4 MPa. While with the addition of hydrogen peroxide from 0.1 wt% to 0.4 wt%, the compressive strength of LWG is in the range of 2.9 MPa to 4.7 MPa.

In the field of geopolymer technology, ASS acts as the gas generation source for producing porous geopolymer or geopolymer foam. ASS reacts with alkali hydroxide and releases gas during the geopolymer curing process, which causes the formation of porosity. Walther *et al.* [40] investigated the use of ASS as a foaming agent to develop a self-foaming geopolymer. The composition included MK, Fly ash, a small amount of Portland Cement, alkaline activators, and ASS. Their results confirm that ASS is effective as a foaming agent for producing geopolymer foams. The foaming reaction completed after 30 min of mixing [40]. Bumanis *et al.* [41] produced geopolymer foam by adding ASS in the range of 10 wt% to 50 wt%. The obtained compressive strength is around 1.5 MPa to 3.8 MPa. Moreover, wastes from the aluminum industry [42,43] and phosphate washing sludge [44] have been utilized as a foaming agent. Although the direct foaming method enables easy pore production, the pore structure cannot be controlled [26]. By adding excessive amounts of foaming agent, large pore size is generated, resulting in low strength of PG [24-26]. Poowancum and Aengchuan [45] have been developed the sequence mixing (SM) method to control the pore generated during geopolymer hardening process. The SM method proceeds by mixing the geopolymer precursor with NaOH and then soaking it for a certain period before adding Na_2SiO_3. The SM method allows for the release of generated gas from the geopolymer before it hardens.

There are numerous research reports on the use of ASS waste as a valuable material. However, the utilization of ASS waste as a foaming agent for the fabrication of PG has never been reported. The aim of this study is to develop the PG by using ASS as a foaming agent. The SM method is applied for fabrication of PG. MK is used as a geopolymer precursor. The solution of NaOH and Na_2SiO_3 is used as the alkali activator solution. The effect of ASS on the properties of PG, and the effective method to utilize ASS as the foaming agent for the fabrication of PG is revealed in this work.

2. Materials and methods

The schematic of the SM methods for fabricating PG is illustrated in Figure 1. The details are as follows:

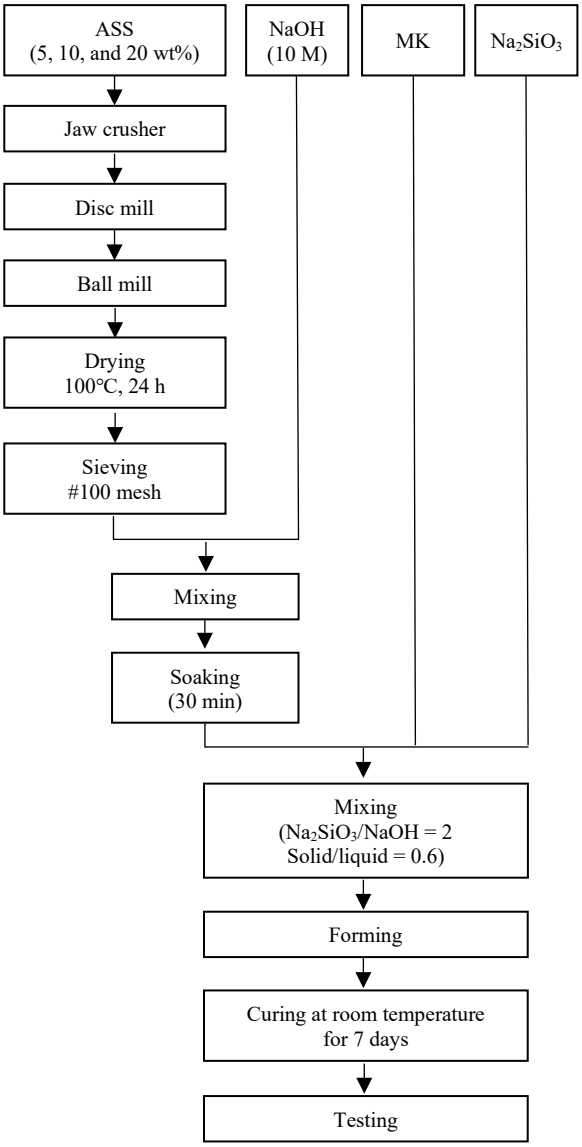

Figure 1. Schematic of the PG fabricating.

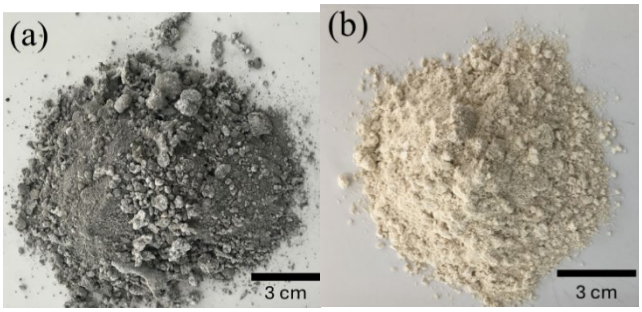

Figure 2. (a) ASS, and (b) MK raw materials.

2.1 ASS preparation

ASS waste from an aluminum alloy melting process obtained from a die casting factory in Thailand (Figure 2(a)) was crushed by a jaw crusher and disc mill, then was milled by a ball mill for 2 h. The milled ASS powder was dried in an oven at 100°C for 2 day and then passed through a 100-mesh sieve (150 µm). Average particle size of the obtained ASS powder was 4 µm as seen in Figure 3.

2.2 Sample preparation

The commercial MK used in this work was supplied by a company in Thailand. MK was chosen as the geopolymer precursor because it is considered one of the most effective materials for synthesizing geopolymers. The SM method is used to prepare PG samples. The 10 M NaOH solution [15] was prepared by dissolving 400 g of the NaOH (99% purity) pellets in 1000 mL of deionized water. After dissolution, the NaOH solution was cooled to room temperature before being introduced to the mixing process. The ASS was mixed with the NaOH solution and soaked for 30 min [40], then MK and sodium silicate (Na_2SiO_3) solution were added. The Na_2SiO_3 used was composed of Na_2O, SiO_2, and H_2O at 16.3%, 34.2%, and 45.5%, respectively.

Average particle size of the commercial MK powder (Figure 2(b)) was 6 µm as demonstrated in Figure 3. Mixing ratios of MK:ASS was 95:5, 90:10, and 80:20 by weight. The ratio of Na_2SiO_3 to NaOH was 2.0 by weight [11]. The solid to liquid ratio was 0.6 by weight [18]. Table 1 shows the compositions of all mixtures. After mixing, the slurry mixture was poured into 50 mm × 50 mm × 50 mm molds. The samples were sealed with a vinyl sheet and were cured at room temperature for 7 day.

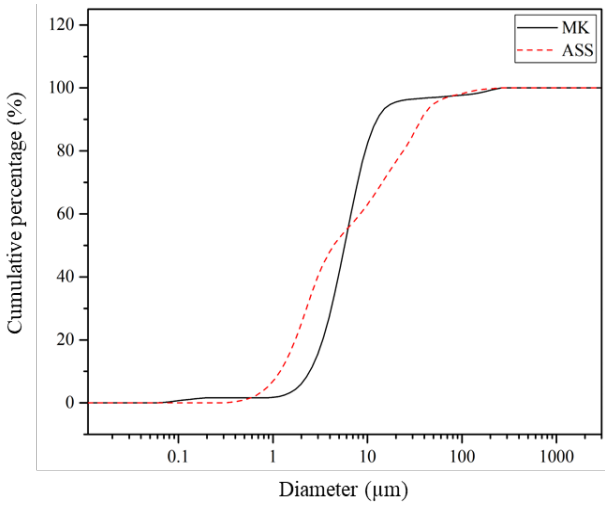

Figure 3. Particle size distribution of ASS after milling process and MK powder.

Table 1. Compositions of mixtures.

Sample	Compositions		Alkali-activator		Solid : liquid (weight ratio)
	MK	ASS	NaOH concentration (molar)	Na_2SiO_3:NaOH (weight ratio)	
PG1	95	5	10	2.0	0.6
PG2	90	10	10	2.0	0.6
PG3	80	20	10	2.0	0.6

2.3 Characterization techniques

Chemical compositions of ASS and MK were examined by X-ray fluorescence (XRF; HORIBA XGT-5200). The phase compositions of ASS were evaluated by X-ray diffraction (XRD; Bruker D2 PHASER). Scanning electron microscopy (SEM; Neoscope JCM-5000) was used to observe the microstructure of PG. The setting time of PG was examined according to ASTM C266 [46]. The initial and final Gillmore needles used were a needle of 113.4 g (diameter of 2.12 mm) and a needle of 453.6 g (diameter of 1.06 mm), respectively. The initial setting time was measured after mixing the sample for 60 s. The initial Gillmore needle was placed on the sample surface. This procedure was repeated every 60 s until the sample surface was no longer marked. The final setting time was evaluated immediately after the initial setting time was determined. The same procedure as the initial setting time measurement was used with the final Gillmore needle. Pore size of PG was measured by using Martin's diameter technique [47]. The sample size for pore size measurement was 200. The porosity (%P) was measured in accordance with ASTM C642 [48] with a sample size of 8 pieces and calculated using the following Equation:

$$\%P = [(M3 - M1)/(M3 - M2)] \times 100 \quad (1)$$

where M1, M2, and M3 are dry weight, immersed weight in water, and wet weight, respectively.

The compressive strength (S) of PG was measured following ASTM C109 [49] using a universal testing machine with a cross-speed of 0.5 mm·min^{-1} and calculated according to the following formula:

$$S = L/A \quad (2)$$

where L is the load at the sample fracture and A is the cross-sectional area of the test specimen. The sample size for testing was 3.

The standard deviation of porosity and pore diameter data was expressed by error bars. The raw data of compressive strength and setting time are demonstrated.

3. Results and discussion

Chemical compositions of MK and ASS are presented in Table 2. The main compositions of MK are Al_2O_3 and SiO_2 in the percent weight of 36% and 59%, respectively. The chemical compositions of ASS compose of Al_2O_3 (62 wt%), Na_2O (12 wt%) and SiO_2 (11 wt%). Small amounts of MgO, K_2O, Fe_2O_3, SO_3, Cl, ZnO and CaO have also been detected. The oxides of K, Ca, and Fe, along with salts such as NaCl and KCl are used in the smelting process for the secondary production of aluminum [50].

Figure 4 shows the XRD pattern of ASS, the peaks of NaCl, $MgAl_2O_4$, Al, KCl, AlN, Si, Al_2O_3 and SiO_2 are detected. The Al and Si contain in ASS are essential components for using as a foaming agent.

Figure 5 shows the variation in the porosity of PG with the addition of ASS. The porosity increases with an increase in the content of ASS. The porosity of PG containing 5%, 10%, and 20% by weight of ASS is 34 ± 2%, 35 ± 1%, and 42 ± 2%, respectively. Porosity of PG is generated through the reaction between Al and Si in ASS with NaOH solution as following Equation (1) - (2) [22].

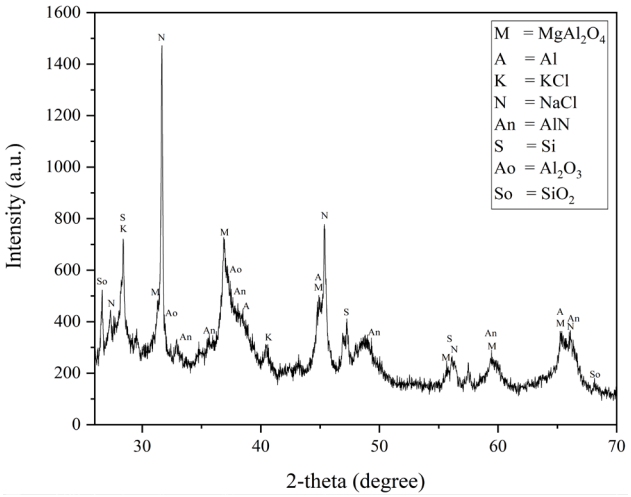

Figure 4. XRD diffractogram of ASS.

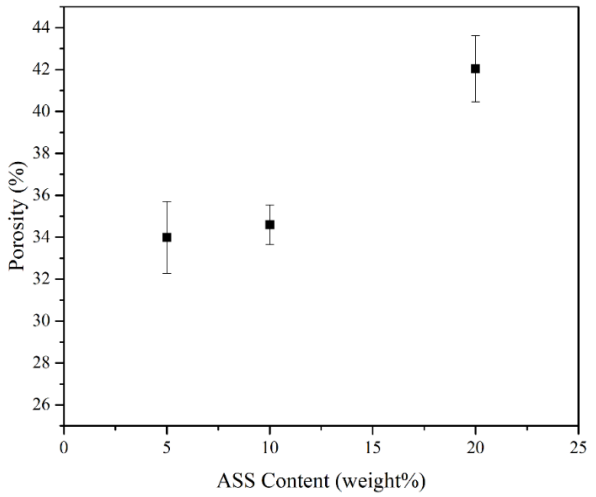

Figure 5. Porosity of the 7 days cured PG with different amounts of ASS addition.

$$2Al + 2NaOH + 2H_2O \rightarrow 2NaAlO_2 + 3H_2(g) \quad (1)$$

$$Si + 2NaOH + H_2O \rightarrow Na_2SiO_3 + 2H_2(g) \quad (2)$$

The generated gas, i.e., H_2, is trapped in the geopolymer during the geopolymer hardening process. An increase in the amount of ASS leads to an increase in the amount of H_2 gas, which results in the high porosity of PG. Typically, by using ASS as foaming agent with the conventional fabrication process, the quantity of porosity cannot be controlled due to lot of gas generated during the geopolymer hardening process [26]. On the other hand, the porosity of PG is controlled by SM. The geopolymer is hardened through the geopolymerization process which is an integrated process involving the dissolution of the geopolymer precursor to form aluminate and silicate species, and the condensation of aluminate and silicate species [51]. NaOH affects the dissolution process, while Na_2SiO_3 influences the condensation process [45]. The dissolution and condensation processes are separated by SM. Therefore, the generated gas is partially released from the geopolymer before it hardens.

Table 2. Chemical compositions of MK and ASS.

Raw materials	Chemical compositions (wt%)										
	Al_2O_3	SiO_2	Na_2O	MgO	SO_3	Cl	K_2O	CaO	Fe_2O_3	ZnO	TiO_2
MK	36	59	0	0	0	0	1	0	2	0	2
ASS	62	11	12	8	2	2	1	1	1	1	0

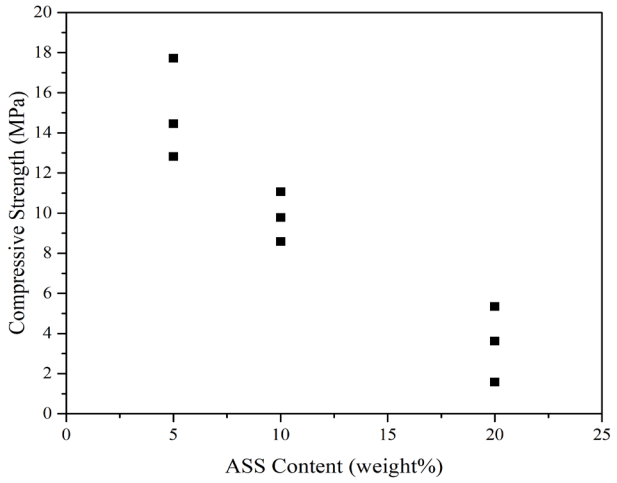

Figure 6. Compressive strengths of the 7 days cured PG with different addition of ASS.

The compressive strength of PG is reduced with an increasing amount of ASS, as seen in Figure 6. Compressive strength is related to porosity. High porosity leads to low compressive strength. Increasing the amount of ASS results in an increase in porosity, which in turn reduces the compressive strength of PG. The compressive strength of PG containing ASS of 5%, 10%, and 20% by weight is 15, 10, and 4 MPa, respectively. The compressive strength of PG containing 5 wt% of ASS is 15 MPa, which is close to the minimum requirement of Portland cement of 19 MPa [52]. This value is sufficient for engineering applications.

The initial and final setting times represent the time for hardening and are the parameters controlling the workability. Figure 7 shows the effect of the ASS content on the setting time of PG, which increases with an increasing amount of ASS. Setting time relates to the rate of the geopolymerization reaction. A lower reaction rate results in a longer hardening time. ASS has a low geopolymerization reaction. Therefore, the time for the hardening of PG is delayed, i.e., the initial setting time is 72 min for the PG containing 5 wt% ASS, whereas it is 127 min for the PG containing 20 wt% ASS. The advantage of delayed setting times is an increase in the working time.

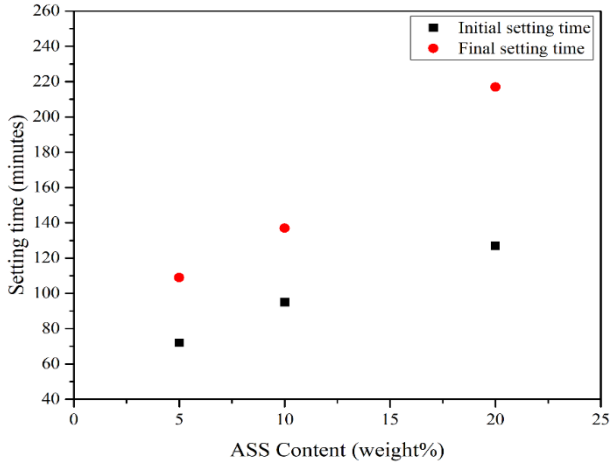

Figure 7. Setting times of PG with different addition of ASS.

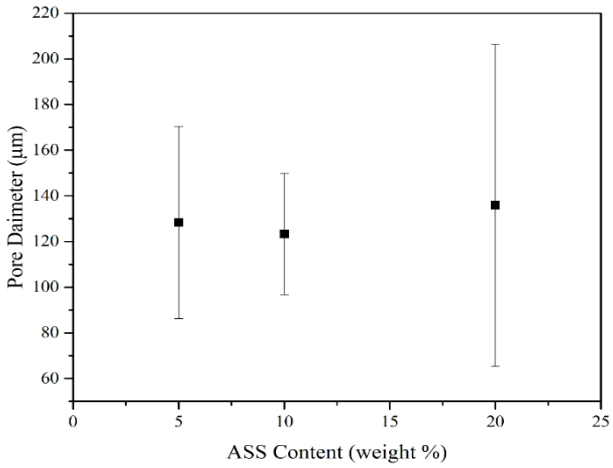

Figure 8. Pore diameters of the 7 days cured PG.

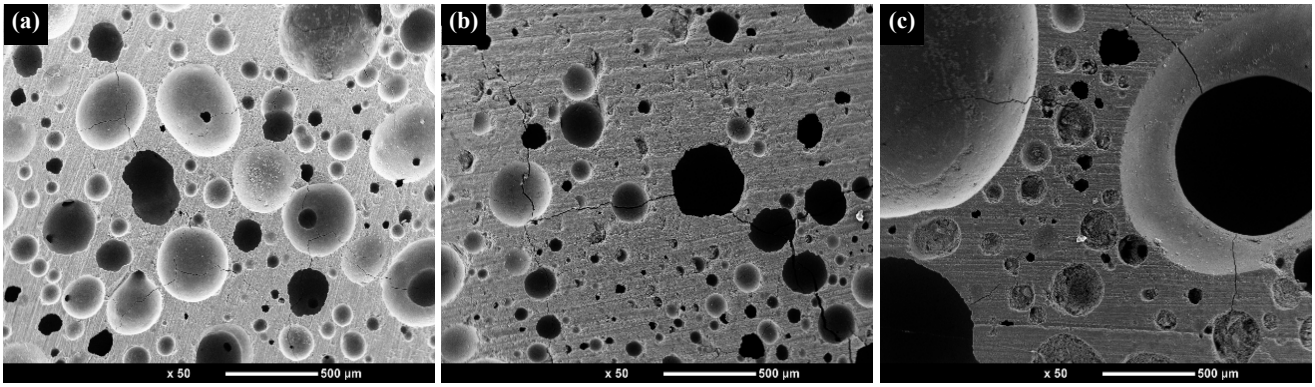

Figure 9. SEM micrograph of the 7 days cured PG containing ASS of (a) 5 wt%, (b) 10 wt%, and (c) 20 wt%.

The pore size of 7 days cured PG are seen in Figure 8. The average pore size of sample contains ASS of 5, 10 and 20 wt% is 128 ± 42, 123 ± 26, and 136 ± 70 μm, respectively. Pore size is increased with increasing of ASS amount. The agglomeration of pores causes the formation of larger pores. The quantity of pores increases with an increase in ASS content (Figure 5). As a result, it agglomerates, and pore size increases, which agrees with the SEM micrograph as seen Figure 9. The SEM micrographs of 7 days cured PG demonstrate that there is the agglomeration of pores, and the pore size is significantly larger in the 20 wt% ASS sample.

4. Conclusions

In the present work, porous geopolymers (PG) have been developed. Aluminum salt slag (ASS) is utilized as the foaming agent, and metakaolin is used as the geopolymer precursor. Sodium hydroxide (NaOH) and sodium silicate (Na_2SiO_3) are used as the alkali activator solution. The sequence mixing (SM) method is essential for the fabrication of PG due to the gas generated from the reaction between ASS and the alkali solution is entrapped in the sample during hardening process. By using SM, the produced gas can be released before the sample hardens. The porosity and compressive strength of PG containing 5 wt% ASS are 34 vol% and 15 MPa, respectively. The compressive strength value is close to the minimum requirement of Portland cement and is useable for engineering applications. ASS influences the setting time of PG, causing an increase in the setting time. Additionally, the pore size of PG increases with higher amounts of ASS.

The knowledge of the present work opens an opportunity to utilize the ASS as a hazardous waste to be a useful material, i.e., a geopolymer-foaming agent, and provides a sustainable solution for managing ASS waste.

Acknowledgements

This research was financially supported by the Suranaree University of Technology Research and Development Fund, and Thailand Science Research and Innovation (TSRI).

References

[1] L. Grande, M. Á. Vicente, S. A. Korili, and A. Gil, "Synthesis strategies of alumina from aluminum saline slags," *Process Safety and Environmental Protection*, vol 172, pp. 1010-1028, 2023.

[2] H. Hao, Y. Geng, and W. Hang, "GHG emissions from primary aluminum production in China: Regional disparity and policy implications," *Applied Energy*, vol. 166, pp. 264-272, 2016.

[3] P. E. Tsakiridis, "Aluminium salt slag characterization and utilization – A review," *Journal of Hazardous Materials*, vol. 217-218, pp. 1-10, 2012.

[4] C. Dai, and D. Apelian, "Fabrication and characterization of aluminum dross-containing mortar composites: Upcycling of a waste product," *Journal of Sustainable Metallurgy*, vol. 3, no. 2, pp. 230-238, 2016.

[5] H. Shen, B. Liu, C. Ekberg, and S. Zhang, "Harmless disposal and resource utilization for secondary aluminum dross: A review," *Science of the Total Environment*, vol. 760, 2021.

[6] A. Meshram, and K. K. Singh, "Recovery of valuable products from hazardous aluminum dross: A review. Resources," *Conservation and Recycling*, vol. 130, pp. 95-108, 2018.

[7] X. Zhu, J. Yang, Y. Yang, Q. Huang, and T. Liu, "Pyro-metallurgical process and multipollutant co-conversion for secondary aluminum dross: A review," *Journal of Materials Research and Technology*, vol. 21, pp. 1196-1211, 2022.

[8] C. Wang, S. Li, Y. Guo, Y. Y. He, J. Liu, and H. Liu, "Comprehensive treatments of aluminum dross in China: A critical review," *Journal of Environmental Management*, vol. 345, p. 118575, 2023.

[9] M. Mahinroosta, and A. Allahverdi, "Hazardous aluminum dross characterization and recycling strategies: A critical review," *Journal of Environmental Management*, vol. 223, pp. 452-468, 2018.

[10] C. Dai, and D. Apelian, "Fabrication and characterization of aluminum dross-containing mortar composites: upcycling of a waste product," *Journal of Sustainable Metallurgy*, vol.3, no. 2, pp. 230-238, 2017.

[11] J. Ayawanna, and A. Poowancum, "Enhancing flexural strength of metakaolin-based geopolymer reinforced with different types of fibers," *Sustainable Chemistry and Pharmacy*, vol. 37, p. 101439, 2024.

[12] T. H. Tan, K. H. Mo, S. H. Lai, and T. C. Ling, "Synthesis of porous geopolymer sphere for Ni(II) removal," *Ceramics International*, vol. 47, no. 20, pp. 29055-29063, 2021.

[13] S. Chokkha, "Effect of fly ash on compressive strength of metakaolin based geopolymer," *Applied Mechanics and Materials*, vol. 873, pp. 170-175, 2017.

[14] Y. Ettahiri, B. Bouargane, K. Fritah, B. Akhsassi, L. Pérez-Villarejo, A. Aziz, L. Bouna, A. Benlhachemi, and R. M. Novais, "A state-of-the-art review of recent advances in porous geopolymer: Applications in adsorption of inorganic and organic contaminants in water," *Construction and Building Materials,* vol.395, p. 132269, 2023.

[15] S. Prasanphan, A. Wannagon, T. Kobayashi, and S. Jiemsirilers, "Reaction mechanisms of calcined kaolin processing waste-based geopolymers in the presence of low alkali activator solution," *Construction and Building Materials*, vol. 221, pp. 409-420, 2019.

[16] B. O. Adeleke, J. M. Kinuthia, J. Oti, and M. Ebailila, "Physico-mechanical evaluation of geopolymer concrete activated by sodium hydroxide and silica fume-synthesised sodium silicate solution," *Materials*, vol.16, no. 6, p. 2400, 2023.

[17] S. H. G. Mousavinejad, and M. Sammak, "An assessment of the effect of Na_2SiO_3/NaOH ratio, NaOH solution concentration, and aging on the fracture properties of ultra-high-performance geopolymer concrete: The application of the work of fracture and size effect methods," *Structures*, vol. 39, pp. 434-443, 2022.

[18] Y. Watanabe, and T. Kobayashi, "Synthesis and characterization of metakaolin-based crystalline phase sodium aluminum silicon

oxide geopolymers using concentrated alkaline medium," *Ceramics International*, vol. 48, no. 24, pp. 37448-37452, 2022.

[19] U. C. C. S. Siciliano, J. Zhao, A. C. C. Trindade, M. Liebscher, V. Mechtcherine, and F. D. A. Silva, "Influence of curing temperature and pressure on the mechanical and microstructural development of metakaolin-based geopolymers," *Construction and Building Materials*, vol. 424, no.19, p.135852, 2024.

[20] J. Liu, X. Shi, G. Zhang, and L. Li, "Study the mechanical properties of geopolymer under different curing conditions," *Minerals*, vol. 13, no.5, p. 690, 2023.

[21] A. Yilmaz, F. N. Degirmenci, and Y. Aygörmez, "Effect of initial curing conditions on the durability performance of low-calcium fly ash-based geopolymer mortars," Boletín de la Sociedad Española de Cerámica y Vidrio, 2023.

[22] C. Bai, and P. Colombo, "Processing, properties and applications of highly porous geopolymers: A review," *Ceramics International*, vol. 44, pp. 16103-16118, 2018.

[23] R. M. Novais, R. C. Pullar, and J. A. Labrincha, "Geopolymer foams: An overview of recent advancements," *Progress in Materials Science*, vol. 109, pp. 100621, 2020.

[24] E. Kamseu, B. Nait-Ali, M. C. Bignozzi, C. Leonelli, S. Rossignol, and D. S. Smith, "Bulk composition and microstructure dependence of effective thermal conductivity of porous inorganic polymer cements," *Journal of the European Ceramic Society*, vol. 32, no. 8, pp. 1593-1603, 2012.

[25] P. Chindaprasirt, and U. Rattanasak, "Characterization of porous alkali-activated fly ash composite as a solid absorbent," *International Journal of Greenhouse Gas Control*, vol. 85, pp. 30-35, 2019.

[26] D. Kioupis, A. Zisimopoulou, S. Tsivilis, and G. Kakali, "Development of porous geopolymers foamed by aluminum and zinc powders," *Ceramics International*, vol. 47, no. 18, 2021.

[27] V. Vaou, and D. Panias, "Thermal insulating foamy geopolymers from perlite," *Minerals Engineering*, vol. 23, no. 14, pp. 1146-1151, 2010.

[28] S. Yan, X. Ren, W. Wang, C. He, and P. Xing, "Preparation of eco-friendly porous ceramic with low thermal conductivity by high-temperature treatment of foamed solid waste based geopolymer with cenospheres," *Construction and Building Materials*, vol. 398, pp. 131190, 2023.

[29] V. Medri, E. Papa, J. Dedecek, H. Jirglova, P. Benito A. Vaccari, and E. Landi, "Effect of metallic Si addition on polymerization degree of in situ foamed alkali-aluminosilicates." *Ceramics International*, vol. 39, no. 7, pp. 7657-7668, 2013.

[30] C. Zoude, L. Gremillard, and E. P. Homme, "Combination of chemical foaming and direct ink writing for lightweight geopolymers," *Open Ceramics*, vol. 16, no.14, p. 100478, 2023.

[31] W. Sornlar, A. Wannagon, and S. Supothina, "Stabilized homogeneous porous structure and pore type effects on the properties of lightweight kaolinite-based geopolymers," *Journal of Building Engineering*, vol. 44, p.103273, 2021.

[32] S. Sanguanpak, A. Wannagon, C. Saengam, W. Chiemchaisri, and C. Chiemchaisri, "Porous metakaolin-based geopolymer granules for removal of ammonium in aqueous solution and anaerobically pretreated piggery wastewater," *Journal of Cleaner Production*, vol. 297, p. 126643, 2021.

[33] N. A. Jaya, L. Y. Ming, H. C. Yong, M. M. A. B. Abdullah, and K. Hussin, "Correlation between pore structure, compressive strength and thermal conductivity of porous metakaolin geopolymer," *Construction and Building Materials*, vol .247, p. 118641, 2020.

[34] J. Fiset, M. Cellier, and P. Y. Vuillaume, "Macroporous geopolymers designed for facile polymers post-infusion," *Cement and Concrete Composites*, vol. 110, p. 103591, 2020.

[35] F. Xu, G. Gu, W. Zhang, H. Wang, X. Huang, and J. Zhu, "Pore structure analysis and properties evaluations of fly ash-based geopolymer foams by chemical foaming method," *Ceramics International*, vol. 44, no. 16, pp.19989-19997, 2018.

[36] X. Liu, C. Hu, and L. Chu, "Microstructure, compressive strength and sound insulation property of fly ash-based geopolymeric foams with silica fume as foaming agent," *Materials*, vol. 13, no. 14, p. 3215, 2020.

[37] D. Wattanasiriwech, K. Yomthong, and S. Wattanasiriwech, "Characterisation and properties of class C-fly ash based geopolymer foams: Effects of foaming agent content, aggregates, and surfactant," *Construction and Building Materials*, vol. 306, p. 124847, 2021.

[38] N. A. Jaya, L. Y. Ming, H. C. Yong, M. M. A. B. Abdullah, and K. Hussin, "Correlation between pore structure, compressive strength and thermal conductivity of porous metakaolin geopolymer," *Construction and Building Materials*, vol. 247, p. 118641 , 2020.

[39] G. Masi, W. D.A. Rickard, L. Vickers, M. C. Bignozzi, and A. V. Riessen, "A comparison between different foaming methods for the synthesis of light weight geopolymers," *Ceramics International*," vol. 40, no. 9, pp. 13891-13902, 2014.

[40] B. Walther, B. Feichtenschlager, and S. Zhou, "Self-foaming Geopolymer Composition Containing Aluminum Dross." United States Patent, US 9580356 B2. 2017.

[41] G. Bumanis, D. Bajare, A. Korjakins, and D. Vaičiukynienė, "Sulfate and freeze-thaw resistance of porous geopolymer based on waste clay and aluminum salt slag," *Minerals*, vol. 12, p. 1140, 2022.

[42] C. Leiva, Y. Luna-Galiano, C. Arenas, B. Alonso-Fariñas, and C. Fernández-Pereira, "A porous geopolymer based on aluminum-waste with acoustic properties," *Waste Management*, vol. 95, pp. 504-512, 2019.

[43] A. Maldonado-Alameda, J. Mañosa, T. López-Montero, R. Catalán-Parra, and J. M. Chimenos, "High-porosity alkali-activated binders based on glass and aluminum recycling industry waste," *Construction and Building Materials*, vol. 400, 2023.

[44] H. Majdoubi, Y. Haddaji, O. Bourzik, M. Nadi, J. Ziraoui, T. S. Alomayri, M. Oumam, B. Manoun, J. Alami, Y. Tamraoui, and H. Hannache, "Enhancing thermal insulation with phosphate washing sludge waste as an inorganic foaming agent in porous acid-based geopolymers: Formulation and processing optimization," *Construction and Building Materials*, vol. 407, 2023.

[45] A. Poowancum, and P. Aengchuan, "Utilization of low reactivity fly ash for fabricating geopolymer materials," *Advances in Cement Research*, vol. 35, no. 3, pp. 1-21, 2022.

[46] ASTM C266-21, "Standard Test Method for Time of Setting of Hydraulic-Cement Paste by Gillmore Needles," *In: Annual*

Book of ASTM Standard, ASTM International, West Conshohocken, PA, USA, 2021.

[47] D. Wang, and L. S. Fan, "Particle characterization and behavior relevant to fluidized bed combustion and gasification systems," In Fluidized Bed Technologies for Near-Zero Emission Combustion and Gasification, pp. 42-76, 2013.

[48] ASTM C642-13, "Standard Test Method for Density, Absorption, and Voids in Hardened Concrete," *In: Annual Book of ASTM Standard, ASTM International, West Conshohocken, PA, USA,* 2013.

[49] ASTM C109/C109M-20, "Standard Test Method for Compressive Strength of Hydraulic Cement Mortars (Using 2-in. or [50-mm] Cube Specimens)," *In: Annual Book of ASTM Standard, ASTM International, West Conshohocken, PA, USA,* 2020.

[50] B. R. Das, B. Dash, B. C. Tripathy, I. N. Bhattacharya, and S. C. Das, "Production of η-alumina from waste aluminium dross," *Minerals Engineering*, vol. 20, no. 3, pp. 252-258, 2007.

[51] E. Nimwinya, W. Arjharn, S. Horpibulsuk, T. Phoo-ngernkham, and A. Poowancum, "A sustainable calcined water treatment sludge and rice husk ash geopolymer," *Journal of Cleaner Production*, vol. 119, pp. 128-134, 2016.

[52] ASTM C150/C150M-20, "Standard Specification for Portland Cement," *In: Annual Book of ASTM Standard, ASTM International, West Conshohocken, PA, USA,* 2020.